Determination of Cloud Vertical Structure from Upper-Air Observations

JUNHONG WANG

Department of Geological Sciences, Columbia University, New York, New York

WILLIAM B. ROSSOW

NASA Goddard Institute for Space Studies, New York, New York

(Manuscript received 25 August 1994, in final form 23 March 1995)

ABSTRACT

A method is described to use rawinsonde data to estimate cloud vertical structure, including cloud-top and cloud-base heights, cloud-layer thickness, and the characteristics of multilayered clouds. Cloud-layer base and top locations are identified based on three criteria: maximum relative humidity in a cloud of at least 87%, minimum relative humidity of at least 84%, and relative humidity jumps exceeding 3% at cloud-layer top and base, where relative humidity is with respect to liquid water at temperatures greater than or equal to 0°C and with respect to ice at temperatures less than 0°C. The analysis method is tested at 30 ocean sites by comparing with cloud properties derived from other independent data sources. Comparison of layer-cloud frequencies of occurrence with surface observations shows that rawinsonde observations (RAOBS) usually detect the same number of cloud layers for low and middle clouds as the surface observers, but disagree more for high-level clouds. There is good agreement between the seasonal variations of RAOBS-determined top pressure of the highest cloud and that from the International Satellite Cloud Climate Project (ISCCP) data. RAOBS-determined top pressures of low and middle clouds agree better with ISCCP, but RAOBS often fail to detect very high and thin clouds. The frequency of multilayered clouds is qualitatively consistent with that estimated from surface observations. In cloudy soundings at these ocean sites, multilayered clouds occur 56% of the time and are predominately two layered. Multilayered clouds are most frequent (≈70%) in the Tropics (10°S–10°N) and least frequent at subtropical eastern Pacific stations. The frequency of multilayered clouds is higher in summer than in winter at low-latitude stations (30°S–30°N), but the opposite variation appears at the two subtropical stations. The frequency distributions of cloud top, cloud base, and cloud-layer thickness and cloud occurrence as a function of height are also presented. The lowest layer of multilayered cloud systems is usually located in the atmospheric boundary layer.

1. Introduction

Cloud vertical structure, including top and base heights, thickness of cloud layers, and the vertical distribution of multilayered clouds affects the large-scale atmospheric circulation by altering gradients of total diabatic heating/cooling composed of the radiative heating/cooling and latent heat release (e.g., Webster and Stephens 1984). A number of numerical experiments and observations have implied a significant role of cloud vertical structure in influencing the general circulation (e.g., Slingo and Slingo 1988; Randall et al. 1989). Tropical studies have shown that the extensive tropical cloud clusters modify the vertical profile of heating sufficiently to alter the large-scale circulation and deep cumulus convection (e.g., Houze 1982).

Comprehensive cloud climatologies are available from surface observations (Hahn et al. 1982, 1984; Warren et al. 1986, 1988) and from the International Satellite Cloud Climatology Project (ISCCP) (Rossow and Schiffer 1991). Neither surface nor satellite observations, however, provide complete information on cloud vertical structure. Surface observers have difficulty identifying middle- and high-level clouds reliably, especially at night or in low overcast conditions, and cannot measure cloud-top height. Satellite observations have an obscured view of low-level clouds and do not provide any information on cloud-base heights. The vertical profiles of temperature and humidity measured by rawinsondes as they penetrate clouds should reflect some aspects of the vertical distribution of clouds because water vapor is saturated or supersaturated in a cloud. However, this source of information on cloud-layer structure has only been used in a few studies (Essenwanger and Haggard 1962; AWS 1979; Starr and Cox 1980).

Poore et al. (1995) (hereafter referred as PWR95) combined rawinsonde and surface observations to create a preliminary climatology of cloud-layer thicknesses. RAOBS (rawinsonde observations) humidity

Corresponding author address: Junhong Wang, Institute for Space Studies, Columbia University, 2880 Broadway, New York, NY 10025. E-mail: ciwxj @ giss.nasa.gov

© 1995 American Meteorological Society

profiles were employed to determine the locations of cloud-layer top and base using the AWS (1979) criteria. Surface observations were used as quality checks and to provide cloud amount and type information. However, as discussed in PWR95, some cloud layers are discarded in the analysis due to the limitations in surface and rawinsonde observations and the required strict agreement between rawinsonde and surface observations, which causes an underrepresentation of some cloud types (mostly middle and high level) and an underestimation of the frequency of multilayered clouds. Possible improvements in the analysis method were suggested in PWR95. Additionally, the climatology in PWR95 has poor ocean coverage; only 14 coastal and 15 island sites are used to represent Northern Hemisphere oceans.

In this study, rawinsonde data at 30 ocean sites (9 ships and 21 islands; Table 1) are studied for three purposes: 1) as a test dataset to develop an improved analysis method that uses RAOBS alone to determine cloud vertical structure, 2) to increase the sampling of multilayered cloud cases, and 3) to check the representativeness of the ocean part of the PWR95 climatology. In section 2, the rawinsonde data and its quality, as well as the revised analysis method, are described. Limitations of RAOBS and the analysis method are discussed in section 3. In section 4, derived cloud vertical structure information is compared with other independent information. To illustrate cloud-layer information that can be developed from RAOBS, we present in section 5 the statistics for these ocean sites, including the frequency of multilayered clouds, the vertical distribution of cloud boundaries (top/base), layer thickness and occurrence, and frequency distribution of separation distances between two consecutive cloud layers in multilayered cloud systems.

2. Data and analysis method

a. Data description

Rawinsonde data at 30 ocean sites (Table 1) were acquired from the National Center for Atmospheric Research. These sites were selected to supplement the ocean coverage of the PWR95 dataset. The geographic distribution of the sites is shown in Fig. 1. Observations are generally taken two times per day at 0000 and 1200 UTC at most sites after 1957; however, observation times are 0300 and 1500 UTC between 1948 and 1957, and 2300 and 1100 UTC prior to 1948.

RAOBS report temperature, humidity, wind speed, and direction as a function of height above mean sea level (MSL) at mandatory, significant, generated, and

TABLE 1. Time records of rawinsonde observations over 30 stations.

Station No.	Station ID	Station name	Latitude	Longitude	Year range
1	2	Ship B	56.30°N	51.00°W	1949–74
2	3	Ship C	52.45°N	35.30°W	1949–73
3	4	Ship D	44.00°N	41.00°W	1949–73
4	5	Ship E	35.00°N	48.00°W	1949–73
5	11	Ship K	45.00°N	16.00°W	1954–69
6	14	Ship N	30.00°N	140.00°W	1949–74
7	17	Ship P	50.00°N	145.00°W	1946–80
8	25	Ship V	34.00°N	164.00°E	1951–72
9	91	Ship T	29.00°N	135.00°E	1950–70
10*	11645	St. Martin	18.03°N	63.07°W	1956–91
11	11647	St. Johns Atg	17.08°N	61.47°W	1957–88
12*	11813	Grand Cayman	19.18°N	81.22°W	1956–91
13	14642	Sable	43.56°N	60.01°W	1958–91
14*	21603	Johnston	16.44°N	169.31°W	1958–84
15*	22701	Midway	28.12°N	177.23°W	1946–91
16	27401	Barter	70.08°N	143.38°W	1953–88
17*	40308	Yap	9.29°N	138.05°E	1951–91
18*	40309	Koror	7.20°N	134.29°E	1951–91
19*	40504	Ponape Caroline	6.58°N	158.13°E	1951–91
20*	40505	Truk Caroline	7.27°N	151.50°E	1951–91
21	40604	Kwajalein Marshall	8.44°N	167.44°E	1952–74
22*	40710	Majuro Marshall	7.05°N	171.23°E	1955–91
23*	41415	Guam Mariana	13.13°N	144.50°E	1952–91
24	41601	Eniwetok Marshall	11.21°N	162.21°E	1949–69
25*	41606	Wake	19.17°N	166.39°E	1948–91
26	42204	Okinawa	26.21°N	127.46°E	1948–71
27	42401	Iwo Jima	24.47°N	141.19°E	1948–67
28*	61705	Pago Pago	14.20°S	170.43°W	1966–91
29*	70701	Diego Garcia	7.18°S	72.24°E	1972–89
30	93116	San Nicolas	33.15°N	119.27°W	1952–83

* 13 stations used in comparison with SWOBS.

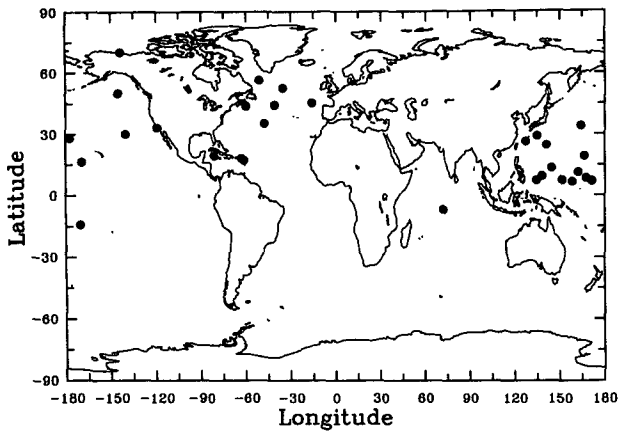

FIG. 1. Geographic distribution of 30 RAOBS sites.

some additional levels (such as the tropopause and maximum wind level) from the surface to the maximum observation altitude. The maximum observation altitude is 10 km on average but varies from sounding to sounding at the same site and from site to site. Humidity is reported as relative humidity (RH) with respect to liquid water at all temperatures.

The frequency of cloud occurrence in layers from one year (July 1983–June 1984) of collocated surface weather observations (SWOBS), obtained from the National Meteorological Center, is compared with that from RAOBS for the same year (section 4a). SWOBS at the same site provide total cloud cover, lower-level cloud amount, standard morphological cloud type, high/middle/low height classes, estimates of the base height above ground level (AGL) of low clouds, and a present weather code (cf. Warren et al. 1986, 1988).

A cloud climatology has been produced from these surface observations (Hahn et al. 1982, 1984; Warren et al. 1986, 1988). We refer to this dataset as SOBS. We use multiyear (1965–76) seasonal mean frequency of co-occurrence of eight cloud types over the ocean from SOBS, which are available over a 15° × 30° (latitude by longitude) grid box, to estimate the frequency of multilayered clouds and compare it with that from RAOBS (section 4c).

Monthly mean cloud-top pressures from collocated ISCCP C2 data from July 1983 to June 1991 are compared with those from RAOBS at 30 sites for all years in which RAOBS are available (Table 1) (section 4b). A detailed comparison of individual cloud-top pressures from the ISCCP C1 data and RAOBS from July 1983 to June 1991 is also shown for two sites (stations 22701 and 40308). The ISCCP C1 data provide cloud amount, top pressure, and optical thickness every 3 h with a spatial resolution equivalent to 2.5° × 2.5° at the equator. The C2 data represent a monthly summary of the C1 data in the form of eight separate monthly averages for each 3-h time period and the average over all diurnal phases (Rossow and Schiffer 1991).

b. Data quality

Problems with RAOBS include shortcomings in the instrument, problematic reporting practices, and data archival problems (Elliott and Gaffen 1991; Gaffen et al. 1991; Schwartz and Doswell 1991). More than 95% of the soundings at the island sites have passed the routine quality tests (hydrostatic and/or consistency checks) made at the National Climatic Data Center (cf. Collins and Gandin 1990), but we found that most of the soundings at the weather ships are not checked. We include the unchecked soundings, but exclude the soundings that are checked and found to be bad.

There are still obvious problems with a small percentage of soundings: 1) negative RH, but with an absolute value less than 20%, 2) no surface level reported, and 3) inconsistency between pressure and height (for instance, the height at 1000 mb is higher than that at 850 mb). The negative RH observations are changed to missing values. The soundings without surface levels are eliminated. In soundings with inconsistencies, we exchange height and/or pressure of the two adjacent levels if the pressure of the higher level is larger than that of the lower one and/or the height of the higher level is smaller than that of the lower one.

Because the RH profile is used to indicate cloud-top and cloud-base locations, more attention must be paid to biases in RH due to instrument errors, reporting practices, and finite vertical resolution. The frequency distribution of RH at U.S. sites (see the example for station 40308 in Fig. 2) shows a spuriously high frequency at 19% caused by the practice of reporting all RH values less than 20% as 19% at U.S. sites after 1973 (Elliott and Gaffen 1991). Figure 2 also shows a sharp drop in the percentage of observations with RH > 96%, which is attributed to the high RH cutoff employed at U.S. sites (cf. Schwartz and Doswell 1991). Vertical resolution varies from sounding to sounding. On av-

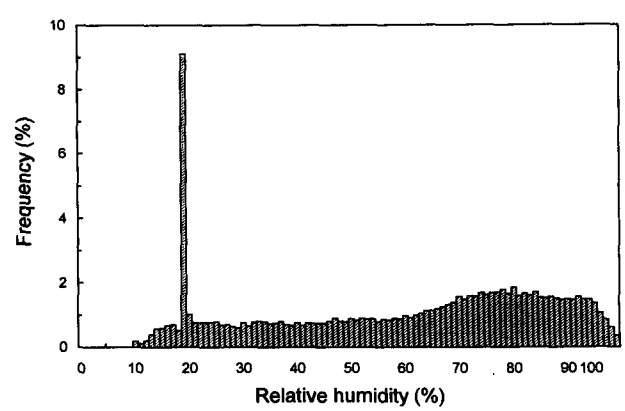

FIG. 2. Frequency distributions of RH at all levels at station 40308.

erage, vertical resolution is 50 mb from the surface to 200 mb, 25 mb from 200 to 100 mb, and 10 mb from 100 to 1 mb, but there is significant interannual variation in vertical resolution. We return to this issue in section 3.

ISCCP cloud-top pressure is derived from cloud-top temperature by using an atmospheric temperature–pressure profile obtained from the TIROS Operational Vertical Sounder (TOVS) produced by the National Oceanic and Atmospheric Administration (Rossow et al. 1991). The TOVS data agree with the RAOBS-based climatology of Oort (1983) to within their estimated uncertainties of 2 K and 25% RH, respectively (Rossow et al. 1991). Uncertainties in cloud-top temperature arise from uncertain calibration (2–4 K) (Brest and Rossow 1992; Klein and Hartmann 1993a), which is equivalent to an uncertainty of top pressures 20–40 mb (height uncertainty about 0.5 km). Larger errors can occur for optically thin cirrus clouds (about 1.5 km in top height) because the ISCCP analysis corrects the emissivity of such clouds using an optical thickness retrieved assuming a cloud composed of 10-μm effective radius water spheres instead of larger ice crystals (Minnis et al. 1993). The comparison of cloud-top pressures from ISCCP and the Stratospheric Aerosol and Gas Experiment (SAGE II) suggests that ISCCP overestimates the pressure of high-level clouds by up to 50–100 mb because of the difference between ISCCP-derived effective cloud top, at which the equivalent infrared radiance is emitted, and SAGE II–determined physical cloud top (Liao et al. 1995b). Larger errors in ISCCP cloud-top locations can occur when the upper-level clouds overlie lower-level clouds. On the other hand, under some circumstances, cloud-top pressures might be underestimated because the ISCCP analysis assumes the cloud to be at the tropopause if the optical thickness is too small to reconcile the observed infrared brightness temperature with any value in the troposphere (Rossow et al. 1991). Liao et al. (1995b) found that this assumption underestimates top pressures of isolated thin clouds in midlatitudes because the actual top is below the tropopause.

c. *Revised RAOBS analysis method*

The revised analysis method is briefly outlined and then the reasons for each step are explained. Cloudy layers are associated with high RH values above some threshold as the rawinsonde penetrates them. Cloud-layer top and base are identified by sudden RH jumps that are positive at the base and negative at the top, respectively.

The analysis method begins by converting RH with respect to liquid water to RH with respect to ice at temperatures below 0°C. Even though ice-phase clouds may form at lower temperatures and higher vapor pressures, these values of RH represent the thermodynamic limit that prevails soon after ice-cloud formation has commenced. The RH profile is examined from the surface to the top to find cloud layers in four steps (see example in Fig. 3).

1) The base of the lowest moist layer is detected as the level that satisfies any one of three conditions: (a) RH $\geqslant$ 87%, (b) if this level is not the surface level, RH at least 84% but less than 87%, and RH increases by at least 3% from the previous (lower) level, or (c) RH $\geqslant$ 84% if this level is the surface level.

2) The next levels above the base are checked and are temporarily considered as being inside a moist layer if RH $\geqslant$ 84% until a level with RH below 84% or the top of the profile is reached.

3) The levels within the moist layer are tested again from the highest level down to the base, and the top of the moist layer is detected as the level that meets any one of three conditions: (a) RH $\geqslant$ 87%, (b) if this level is not the top of the profile, RH is at least 84% but less than 87%, and there is at least a 3% RH increase from the previous (higher) level, or (c) RH $\geqslant$ 84% if this level is the top of the profile.

4) If a top is not found in step 3, the moist layer is not considered to be a cloud layer. If a top is found, the maximum RH in the layer is found. The detected moist layer is finally judged to be a cloud layer only if the maximum RH is above 87%. Here 87% and 84% are called the maximum and minimum RH thresholds in a cloud, respectively. Searching for other moist layers continues from the level where we stop in step 2 until the top of profile is reached. For cloud layers starting from the ground, a 500-m base height AGL is assigned, unless the top is found to be lower than 500 m, in which case the layer is discarded. For "single-level" clouds, which have the same level identified as top and base, cloud-layer top is assigned at half the distance to the next level above and base is at half the distance to the next level below.

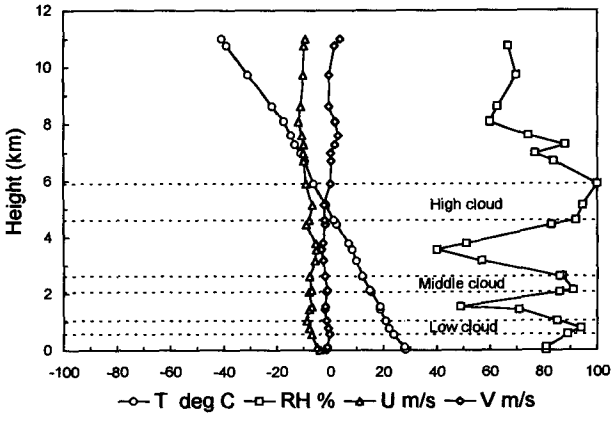

FIG. 3. The profiles of temperature (T), relative humidity (RH), and wind speed (U and V) at station 40308 on 3 January 1984. Three cloud layers are marked corresponding to the RH profile. SWOBS report low, middle, and high clouds and the base height of low cloud in the range 600–999 m.

In SWOBS, the base height of the lowest cloud (stratus, cumulus, or cumulonimbus) is sometimes measured, but in most of the reports it is estimated subjectively (Warren et al. 1986, 1988). Base height is reported as a code from 0 to 9, which corresponds to 10 AGL height intervals: 0–49 m, 50–99 m, 100–199 m, 200–299 m, 300–599 m, 600–999 m, 1000–1499 m, 1500–1999 m, 2000–2499 m, and 2500 m or higher. From one year of individually matched RAOBS and SWOBS, we find that the frequency distribution of RH within the cloud-base intervals determined by SWOBS shows a notable frequency at RH values above 87% with a peak at 95% (Fig. 4), which was used to select our RH thresholds. The drop at RH > 95% is caused by the high RH cutoff employed in the RAOBS analysis. The average dispersion of RH in the cloud-base height intervals, defined as the difference of the maximum and minimum RH, is very small (3%), with 91% of the cases having dispersions less than 10%. Therefore, the existence of clouds with low RH (<84%), the remaining 25% of total cases in Fig. 4, may result mainly from errors in SWOBS-estimated base heights rather than from RH variation within base height intervals. It is also possible that the rawinsonde could pass through a gap in broken or scattered clouds, such as cumulus, and thereby record low RH when SWOBS indicate clouds.

In PWR95, different RH thresholds were applied in three temperature ranges, above 0°C, from 0° to −20°C, and below −20°C, to account for both the difference of RH with respect to liquid water and ice and the underestimation of RH by RAOBS (see section 3). In our revised analysis method, however, we convert RH with respect to liquid water to RH with respect to ice at temperatures below 0°C and use only one RH threshold at all temperatures. It is possible that liquid water still exists at temperatures below 0°C: limited observations show a transition from liquid to ice occurring anywhere between −4° and −40°C (Feigelson 1978; Hobbs and Rangno 1985; Sassen et al. 1989; Curry et al. 1990). In the part of a cloud where supercooled liquid water and ice coexist, the true RH is somewhere between RH with respect to liquid and to ice, depending on the ratio between the quantities of supercooled water and ice, which is unknown. On the other hand, as discussed in the next section, the systematic faults of the humidity element, such as thermal lag, lead to measurements that are lower-than-actual RH values, which worsen with decreasing temperature. Thus, the potential overestimate of RH at warmer temperatures (−10° to 0°C) by converting RH with respect to liquid water to RH with respect to ice, is of the same magnitude as the systematic underestimates of RH in RAOBS. For instance, RH with respect to ice is 4% larger than RH with respect to liquid water at −4°C, but the underestimate of RH from insolation heating and thermal lag can reach 6% at 700 mb and 23% at 250 mb (Pratt 1985).

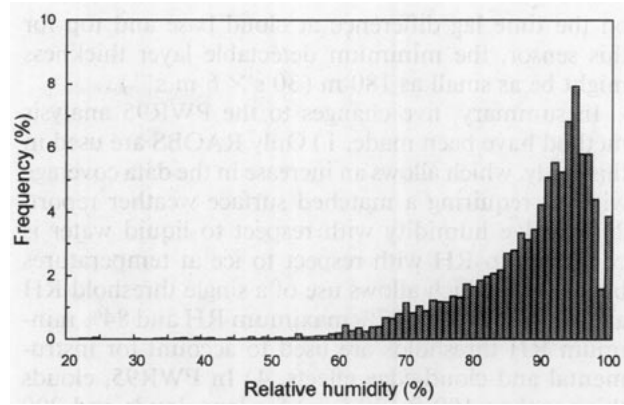

FIG. 4. Frequency distribution of RH within the cloud base interval estimated by SWOBS at 13 sites in one year (July 1983–June 1984).

In about one-quarter of the cloudy RAOBS soundings matched with one year of SWOBS, the lowest RAOBS cloud base is at the ground. Such cases may represent fog, drizzle, or rain below a cloud or a false cloud layer, since RH can be larger than 87% near the surface without the formation of clouds, especially in the Tropics. Among these cases, 16% of them are associated with SWOBS reports of rain, 16% with precipitation, fog, ice fog, or thunderstorms during the preceding hour but not at the time of observation, less than 1.2% with fog and drizzle, 36% with no present weather report, and 32% with a change of the sky state during the past hour. In all these cases, low clouds are reported by SWOBS with a mean base height of 512 m ± 148 m (calculated using the midpoints of SWOBS-estimated base height intervals). Therefore, we keep all such cloud layers with tops above 500 m and assign a 500-m base height AGL.

Single-level clouds, about 20% of the RAOBS-detected cloud layers, are retained in our analysis because they may be produced by the combination of the rawinsonde coarse vertical resolution (from 30 to 50 mb) and the time lag of the rawinsonde humidity elements. Moreover, comparisons of RAOBS results with both SWOBS and ISCCP in section 4 suggest that single-level clouds might be real clouds. For the U.S. lithium chloride humidity element used before 1965, the time lag is the largest (up to 165 s) when a rawinsonde moves from warm, dry air to cooler, moister air (this is usually the case of the rawinsonde entering a moist layer or cloud), but decreases to 10–20 s when the rawinsonde emerges from a cloud or a moist layer into a drier layer above (Bunker 1953). Taking a balloon ascent rate of 6 m s^{-1}, a total 150-s lag difference at cloud base and top implies that cloud layers thinner than 900 m may either be missed or detected as single-level clouds. For the carbon hygristor used at U.S. sites after 1965, the time lag is much shorter than that of the lithium chloride sensor and is less than 30 s at temperatures above −30°C (Pratt 1985). Although there is no information

on the time lag difference at cloud base and top for this sensor, the minimum detectable layer thickness might be as small as 180 m (30 s × 6 m s^{-1}).

In summary, five changes to the PWR95 analysis method have been made. 1) Only RAOBS are used in this study, which allows an increase in the data coverage without requiring a matched surface weather report. 2) Relative humidity with respect to liquid water is converted to RH with respect to ice at temperatures below 0°C, which allows use of a single threshold RH at all levels. 3) Both 87% maximum RH and 84% minimum RH thresholds are used to account for instrumental and cloud-edge effects. 4) In PWR95, clouds thinner than 100 ft (30.5 m) for low clouds and 200 ft (61.0 m) for middle and high clouds were discarded, while all cloud layers, including single-level clouds, are retained in this study. 5) Cloud layers ending at the maximum observation altitude, which were discarded in PWR95, are kept in our analysis. The top heights and layer thicknesses for such clouds are underestimated, however.

3. Analysis sensitivity

Cloud is characterized by RH ≈ 100%; however, 100% RH is rarely observed by rawinsondes penetrating clouds because of 1) systematic biases of rawinsonde measurements discussed below, 2) the high RH cutoff mentioned in section 2, and 3) the fact that RH is always calculated with respect to the liquid phase at all temperatures, which is smaller than RH with respect to ice at temperatures below 0°C. All three factors imply the underestimation of RH in RAOBS. Accordingly, a cloud can exist at a measured RH less than 100%. On the other hand, it is also possible that no cloud exists when RH is high because other factors such as vertical motion also play a role in cloud formation. We present some evidence that there are very few moist but cloud-free layers except near the surface.

The rawinsonde humidity elements measure RH directly, but the thermal lag leads to lower-than-actual RH reports by about 3% as a result of about 1°C above the ambient temperatures inside the hygristor element (Garand et al. 1992). There are additional systematic biases induced by instrument and reporting practice changes. Elliott and Gaffen (1991) have shown that introduction of a new housing with the new carbon hygristor and the method of reporting of low relative humidities, begun in 1965, lead to apparent biases in RH. The introduction of the new housing induces underestimation of RH in daytime, but this factor is less important in our results because most of the stations we use either had more than 85% night observations in 1965–72 or had observation times (0000 and 1200 UTC) that are in the early morning and evening hours. The bias from the new housing has been corrected since 1972. Since we are interested in high values of RH, it is not necessary to consider the effect of the new method of reporting RH values below 20% except for overall quality control.

The average vertical resolution of RAOBS changed by 20 mb (from 50 to 30 mb) around 1970 at all sites except at stations 17, 91, 40604, and 42204. At Sable Island (station 14642 in Table 1), which is operated by Canada, the change in mean vertical resolution (from 50 to 20 mb) happened around 1980. Although no literature has discussed this change, we think that the improvement of vertical resolution is caused by the reporting of RH values below 20% starting from 1965 and/or the increase of generated levels in the archived data in the U.S. radiosonde network. At Canadian station 14642, the resolution change might be associated with the change of humidity algorithm around 1978, which allows computations of humidity for all temperatures above −65°C rather than −40°C used previously (Gaffen 1993). The change in vertical resolution results in a 28% increase in the occurrence of multilayered clouds after 1970.

When the RH thresholds are increased by 3% without a change of RH jump criteria, 15% of the cloud layers disappear and 3% are broken into two or more layers, decreasing the frequency of multilayered clouds by 4%. Top and base heights and layer thicknesses are unchanged for three-quarters of the remaining cloud layers. The average top height MSL decreases by 73 m, base height MSL increases by 68 m, and clouds become thinner by 141 m. About 95% of the cloud layers that disappear are thinner than 1 km. Similar results with opposite signs are found as the RH thresholds are decreased by 3%. When the jump requirement is increased to 6% from 0% without change of maximum and minimum RH thresholds, 3% of the cloud layers disappear and the frequency of multilayered clouds decreases by 1%. For 92% of the remaining cloud layers, top and base heights and layer thicknesses are unchanged. The average changes of top and base heights MSL and layer thickness are −20, 17, and −36 m, respectively. The clouds that disappear are thinner than 1 km. Thus, the changes in RH thresholds and jump size induce only minor variations in cloud-top and cloud-base heights, layer thickness, and frequency of multilayered clouds.

4. Evaluations

a. Comparing cloud occurrence and base height with SWOBS

SWOBS report the occurrence of high, middle, and low clouds, which can be compared with coincident and collocated RAOBS. One year (July 1983–June 1984) of data from both SWOBS and RAOBS are available at 13 sites (Table 1). RAOBS-determined cloud layers are labeled as high, middle, and low clouds according to the layer base height AGL: bases at or below 1981 m (6500 ft) are called low clouds, between 1981 and 5029 m (16 500 ft), middle clouds, and above

5029 m, high clouds (PWR95). Table 2 presents the percentages of matched and mismatched individual RAOBS and SWOBS in the three height categories for five experiments. Matched cases are those in which both RAOBS and SWOBS do or do not report a cloud layer in the same height category; mismatched cases are those in which either RAOBS or SWOBS report a cloud layer in a particular height category but the other does not. Note that the lack of clear sky is a feature of these particular statistics that is not generally representative. The criteria used in the first experiment became our standard (87% maximum and 84% minimum thresholds and 3% jump), except that single-level clouds are excluded. In this case there are 90%, 71%, and 53% of matched cases for low, middle, and high clouds, respectively, indicating that RAOBS usually can detect the same number of cloud layers in the low and middle cloud categories as SWOBS.

We explore four factors that may explain some of the mismatches in layer cloud reports: 1) misclassification of cloud-base height in SWOBS, 2) nighttime effects on SWOBS, 3) obscuration of upper cloud layers by lower layers in SWOBS, and 4) scattered thin cloud layers missed by RAOBS. Considering the first factor, the ground observer's classification of cloud by base height becomes less accurate for upper-level clouds; in fact, the distinction between middle and high clouds may be largely morphological. We also calculated the match-up statistics for only two base height categories, low and other, and found that the percentage of matches is approximately the average of the middle and high matches shown in Table 2. Thus, this factor does not seem important.

The second and third experiments in Table 2 divide the comparison into day-only and night-only observations. Note that the twice-daily sampling and mixture of longitudes in this particular collection of sites may obscure actual diurnal variations. These results show significantly more reports of middle (17%) and high (31%) clouds by SWOBS in daytime, where 17% and 31% are the differences of the sum of M2 and S in Table 2 between daytime and nighttime for middle- and high-cloud categories, respectively. RAOBS only detect about 7% of the extra middle clouds and 5% of the extra high clouds, where 7% and 5% are the differences of M2 in Table 2 between daytime and nighttime for middle and high clouds, respectively. About 10% of the additional middle clouds and 26% of the additional high clouds are missed by RAOBS, decreasing the percentages of matches. However, the fourth experiment shows that, if we include single-level clouds, the RAOBS detect an additional 5% and 11% of middle and high clouds that were missed by RAOBS before. Thus, including single-level clouds improves the match-up statistics, particularly for high clouds, even though we can only determine upper limits on the layer thickness for these cases.

Middle and high clouds can be obscured by low clouds when low cloud cover is large or complete in SWOBS. At 80% of the RAOBS sounding times, the coincident SWOBS indicate a lower-level cloud amount less than 50%. In SWOBS reports, the lower-level cloud amount is usually the amount of all low clouds present, but it can be the amount of middle clouds if there is no low cloud (Warren et al. 1982). Hence, SWOBS should generally be able to detect high clouds. Figure 5 shows that whenever RAOBS report high clouds but SWOBS do not, 59% of these soundings have total cloud cover equal to lower cloud cover, which means that the surface observer cannot see any high clouds that are present. The frequency distribution, however, is more uniform when SWOBS report high clouds but RAOBS do not (Fig. 5). Note that the large number of soundings with zero difference in the matched cases is due to reports of no high clouds in both SWOBS and RAOBS. We conclude that the small

TABLE 2. Comparison of cloud occurrence from RAOBS and SWOBS: Num is the number of samples; M1 is the percent of matched cases in which neither RAOBS nor SWOBS report clouds coincidentally; M2 is the percent of matched cases in which both RAOBS and SWOBS report clouds coincidentally; S is the percent of the cases in which SWOBS report clouds, while RAOBS do not; R is the percent of the cases in which RAOBS report clouds, while SWOBS do not. Total is 100% for each cloud type and each experiment.

	Low clouds					Middle clouds					High clouds				
Experiment	Num	M1	M2	S	R	Num	M1	M2	S	R	Num	M1	M2	S	R
1	4329	<1	90	10	<1	4070	53	18	21	8	3350	32	20	44	4
2	2901	<1	90	10	<1	2769	49	20	25	6	2325	25	22	52	1
3	1428	<1	90	9	<1	1301	60	13	15	12	1025	49	17	26	8
4	4329	<1	96	4	<1	4070	47	23	16	14	3350	30	31	33	6
5	4329	<1	90	10	<1	4070	52	20	20	8	3350	30	28	37	5

Note: Descriptions of experiments 1–5

1) The maximum and minimum RH thresholds are 87% and 84%. Relative humidity jump is 3%. Relative humidity is with respect to ice.

2) The same as experiment 1 except only for daytime cases.

3) The same as experiment 1 except only for nighttime cases.

4) The same as experiment 1 but including single-level clouds.

5) The same as experiment 1 but the maximum and minimum RH thresholds are reduced by 10% and no RH jump is required at temperatures below 0°C.

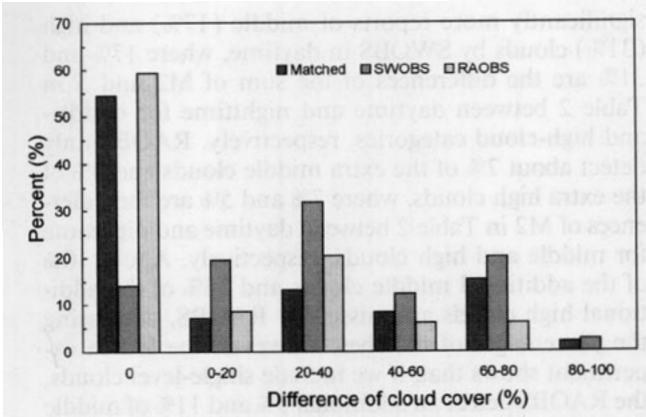

FIG. 5. The frequency of cases as a function of the difference between total and lower cloud cover in the comparison of SWOBS and RAOBS for high cloud category. "Matched" is for matched cases where SWOBS and RAOBS do or do not report clouds coincidentally, "SWOBS" is for the cases in which SWOBS report high cloud while RAOBS do not, and "RAOBS" is for the cases in which RAOBS report high cloud while SWOBS do not.

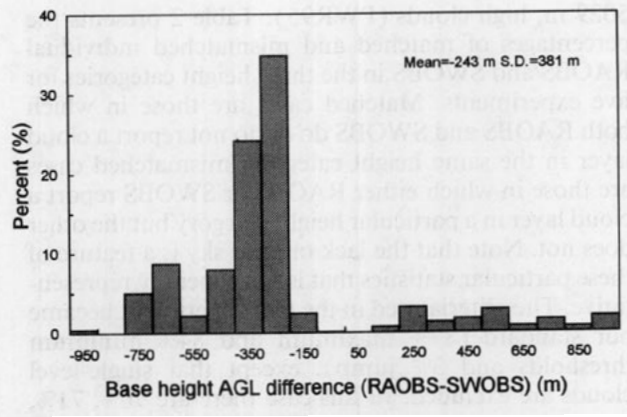

FIG. 6. Frequency of cases as a function of the difference of lowest cloud-base height AGL from RAOBS and SWOBS (RAOBS minus SWOBS) for the cases in which the RAOBS-determined base is not within the SWOBS-estimated base intervals. The central value of the 100-m interval is shown in horizontal axis.

number of cases where RAOBS detect a cloud layer but SWOBS do not are caused by obscuration of upper layers.

Table 2 shows that RAOBS miss 44% of high clouds that are observed by SWOBS (experiment 1); adding single-level clouds reduces this missed fraction to 33% (the fourth experiment in Table 2). Half of those missed high clouds are classified as cirrus fibratus in SWOBS. Rawinsondes may often miss this kind of cloud because such cirrus are in the form of filaments, strands, or hooks and do not cover the whole sky. In addition, the top limit of the RAOBS profile eliminates some very high cloud layers as discussed in section 4b. To test whether the missed high clouds in RAOBS are due to our analysis scheme, in experiment 5 we reduce both the maximum and minimum RH thresholds by 10% and require no RH jump at cloud top and base at temperatures below 0°C. There is no significant improvement on matched percentages for middle and high clouds (72% and 58%, respectively) in comparison to the first experiment in Table 2.

RAOBS-determined base height AGL of the lowest cloud is also compared with that estimated by SWOBS. In 35% of 3995 cases, the RAOBS-determined base is within SWOBS-estimated base intervals. In 78% of the remaining cases, the RAOBS-determined base is within 500 m of the center of the SWOBS-estimated base height intervals, with an average difference of −243 m ± 381 m (Fig. 6).

b. *Comparing cloud-top pressure with ISCCP*

Multiyear monthly mean cloud-top pressures from collocated ISCCP C2 data from July 1983 to June 1991 are compared with those from RAOBS at the 30 sites for all available years (Table 1). Figure 7 displays the comparisons of annual mean cloud-top pressure. (Note that single-level clouds are excluded in RAOBS here.) The two datasets have a correlation coefficient of 0.58 (above the 99% confidence level) with an average difference (RAOBS minus ISCCP) of 87 mb, but the differences are as much as 250 mb in the tropical western Pacific (station numbers from 17 to 24 in Fig. 7). Figure 8 presents two examples of the comparison of seasonal variations of cloud-top pressures from RAOBS and ISCCP at two sites. At all sites, cloud-top pressures from RAOBS and ISCCP have similar seasonal variations; for example, cloud top is lower in summer than in winter at the extratropical eastern Pacific station 14, while the opposite is found at the tropical western Pacific station 40308 (Fig. 8).

To explore the reasons for the larger discrepancies in the tropical western Pacific, individual cloud-top pressures from ISCCP C1 data are compared with those

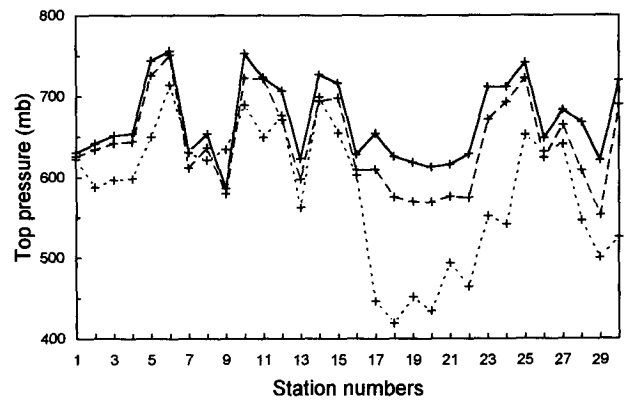

FIG. 7. Comparisons of annual mean cloud-top pressure from RAOBS (solid line) and ISCCP (dotted line) at 30 sites. The dashed line is from RAOBS after adding single-level clouds.

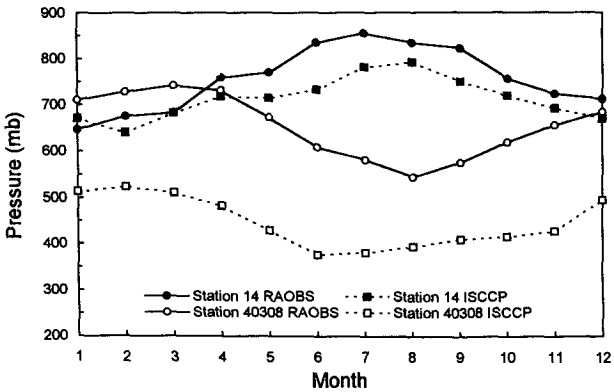

FIG. 8. Comparisons of seasonal variations of cloud-top pressure from RAOBS and ISCCP at stations 14 and 40308.

from individual RAOBS at the same time (0000 UTC), day, month, and year (July 1983–June 1991) at the tropical western Pacific station 40308 and the extratropical eastern Pacific station 22701. Figure 9 shows the frequency distribution of differences of cloud-top pressures from RAOBS and ISCCP. (Note that single-level clouds are also excluded here.) At station 22701, the difference distribution is symmetric about zero with a mean value of 21 mb and a standard deviation of 198 mb, but at station 40308 there are higher frequencies of positive differences and the mean RAOBS value is 198 mb higher with a standard deviation of 225 mb.

The disagreement of cloud-top pressures from RAOBS and ISCCP could be caused, in part, by spatial inhomogeneity of cloud-top pressure over an ISCCP grid cell because RAOBS only observe clouds at one point, whereas the ISCCP-derived top pressure is the average top pressure over a 280-km grid cell. The standard deviation of ISCCP cloud-top pressures in a grid cell is computed from the number of cloudy pixels (pixel is about 30 km) in seven cloud-top pressure categories in C1 data (Rossow et al. 1991). The standard deviation[1] reaches a minimum value at differences near zero, increases with the absolute difference, and peaks at the differences of −250 and 450 mb (Fig. 10).

To test this effect further, we restrict the comparison to cases with the ISCCP cloud cover fraction larger than 50% in any one of seven cloud layers defined by cloud-top pressure (cf. Fig. 4 in Rossow and Schiffer 1991). For these selected cases, there are still higher frequencies of positive differences at station 40308 (Fig. 11); however, the frequency distribution for low/middle and high clouds, shown in Fig. 12, indicates that the extra population of positive differences is for high clouds.

When we add single-level clouds to the RAOBS results, the differences of annual mean top pressures between RAOBS-derived and ISCCP C1 cloud-top pressures at the tropical Pacific stations decrease by about 50 mb (Fig. 7). At station 40308 the mean difference with ISCCP C1 decreases by 59 mb and the population of clouds in the large positive difference regime also decreases significantly in comparison to Fig. 11 (not shown).

In the large negative difference regime, most of clouds are reported to be multilayered by RAOBS, in contrast to the small difference regime (see example for station 22701 in Fig. 13). Thus, these larger negative differences suggest that ISCCP obtains higher cloud-top pressures than RAOBS for multilayered clouds (cf. Liao et al. 1995b); the average overestimate is about 61 mb in about half of the multilayered cases.

The remaining overestimation of high cloud-top pressures in RAOBS is attributed to the top limit of the RAOBS profiles, which can eliminate some very high cloud layers or cause the overestimation of cloud-top pressures for cloud layers that extend above the RAOBS

[1] The values shown are determined from daytime ISCCP results, which correct cloud-top locations using measured cloud optical thickness values; treating all clouds as blackbody emitters reduces the standard deviation by about 30%–40%.

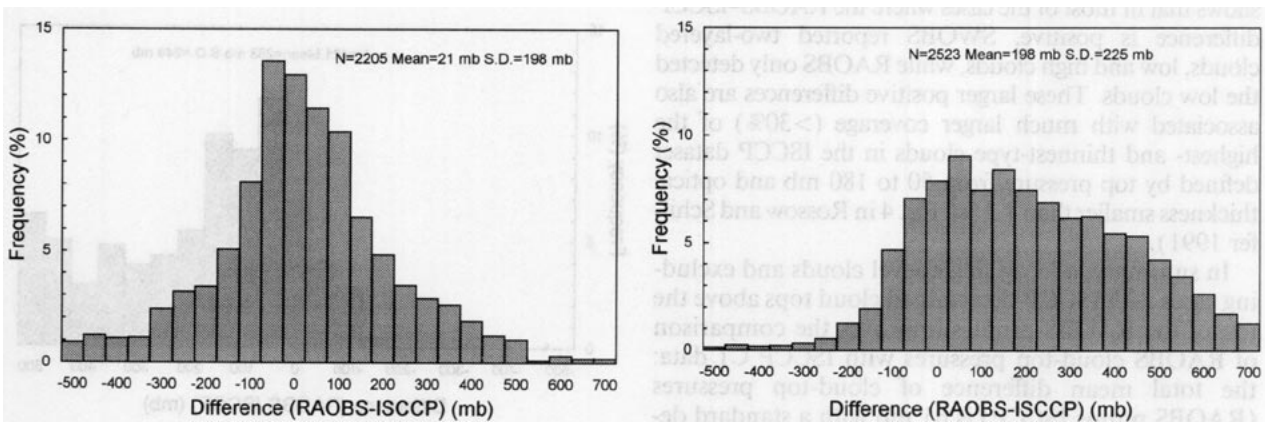

FIG. 9. Frequency distributions of difference in cloud-top pressure from RAOBS and ISCCP at station 22701 (a) and 40308 (b): N is number of samples, mean is average difference (mb), and SD is standard deviation of difference (mb).

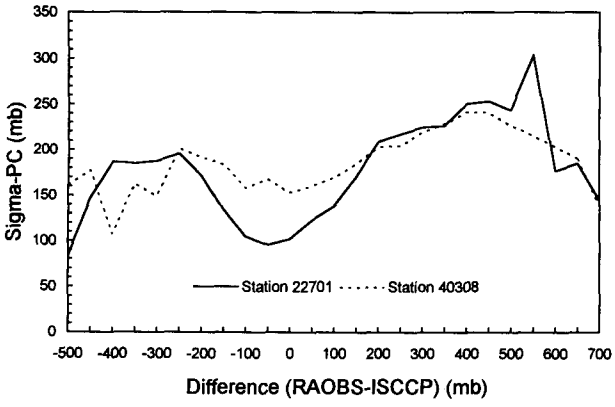

FIG. 10. Variation of standard deviations of cloud-top pressure in an ISCCP grid cell with difference in top pressure from RAOBS and ISCCP at station 22701 and 40308.

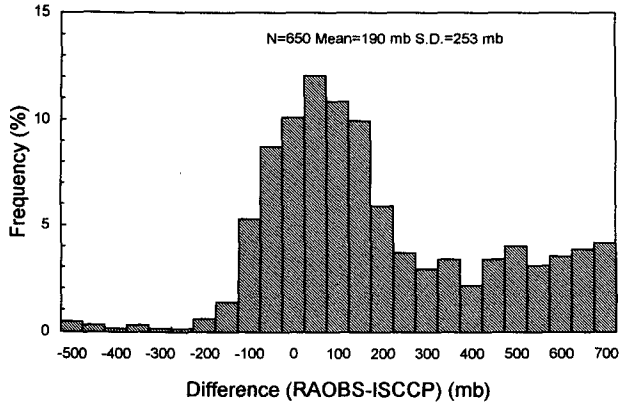

FIG. 11. As in Fig. 9b but for the cases with the cloud cover fraction of any one of seven cloud types defined by cloud-top pressure larger than 50%.

maximum observation altitude. Note that the larger differences of annual mean top pressures in the tropical western Pacific shown in Fig. 7 are also associated with a much higher frequency of cirrus clouds in the ISCCP results (Fig. 14). Typical cirrus base heights (10–14 km) at low latitudes (Heymsfield 1993) are higher than the average RAOBS maximum observation altitude (around 10 km) at most sites. Moreover, at such high altitudes, the temperatures in cirrus cloud can be as low as −50° to −65°C at high midlatitudes (Ansmann et al. 1993). At temperatures below −40°C, however, the rawinsonde humidity element is less reliable and humidity is often reported as missing in current National Weather Service practice (Elliott and Gaffen 1991). After excluding cases with ISCCP-determined cloud tops above the top of the RAOBS profiles in comparison with ISCCP C1 data, the population of cases with larger positive pressure differences is significantly reduced and the mean difference of cloud-top pressures between RAOBS and ISCCP shown in Fig. 11 is decreased by 70 mb. Comparison of cloud occurrence from RAOBS and SWOBS at tropical western Pacific station 40308 in one year (July 1983–June 1984) shows that in most of the cases where the RAOBS–ISCCP difference is positive, SWOBS reported two-layered clouds, low and high clouds, while RAOBS only detected the low clouds. These larger positive differences are also associated with much larger coverage (>30%) of the highest- and thinnest-type clouds in the ISCCP dataset defined by top pressure from 50 to 180 mb and optical thickness smaller than 1.3 (cf. Fig. 4 in Rossow and Schiffer 1991).

In summary, adding single-level clouds and excluding cases with ISCCP-determined cloud tops above the top of the RAOBS profiles improves the comparison of RAOBS cloud-top pressures with ISCCP C1 data: the total mean difference of cloud-top pressures (RAOBS minus ISCCP) is 61 mb with a standard deviation of 228 mb. The mean difference for low/middle clouds and high clouds is −16 and 180 mb, respectively.

c. *Comparing cloud overlap statistics with surface observations*

Using SOBS data described in section 2a, we estimate the frequency of single-layered clouds and compare it with this dataset (Fig. 15). The rawinsonde data after 1970 are employed in Fig. 15 to avoid the effect of the

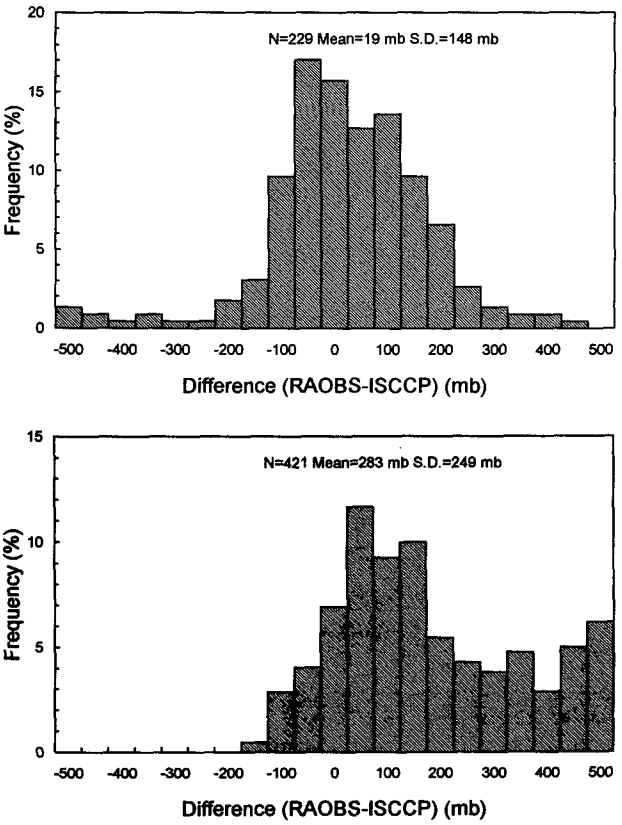

FIG. 12. As in Fig. 11 but for (a) low and middle clouds and (b) high clouds.

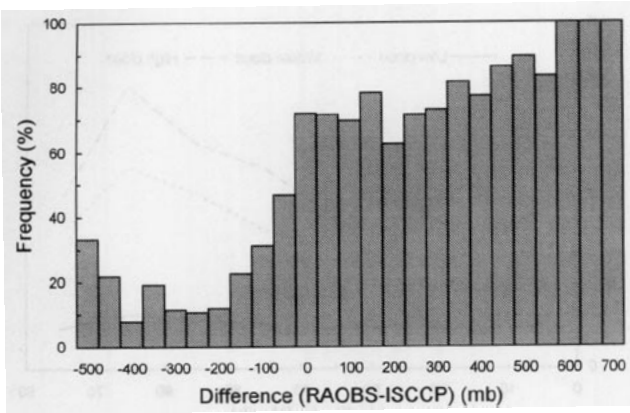

FIG. 13. Frequency of occurrence of single-layered clouds as a function of difference in top pressure from RAOBS and ISCCP at station 22701.

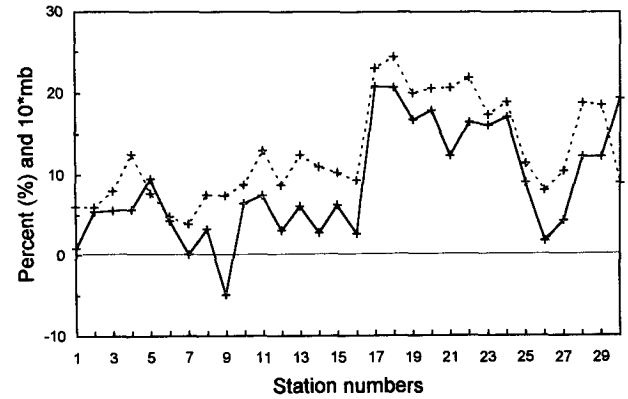

FIG. 14. Comparisons of annual mean cloud-top pressure difference from RAOBS and ISCCP (RAOBS minus ISCCP) (solid line) and the frequency of occurrence of cirrus clouds from ISCCP (dotted line) at 30 sites.

vertical resolution change on the frequency of multilayered clouds (discussed in section 5a). The two datasets agree well both in pattern and magnitude with a correlation coefficient 0.59 (above the 99% confidence level). However, significant disagreement exists at the weather ships (station numbers 1–9 in Fig. 15). One factor affecting this comparison may be that the SOBS ocean statistics are aggregated with a horizontal resolution of 15° × 30° (latitude by longitude) and are derived from all available ships in this area, whereas the RAOBS are from single ships at fixed locations. The disagreement at the ship stations might also be associated with a lower percentage of ship reports contributing to the statistics of the high-level clouds in SOBS (Fig. 15), because of the fundamental assumption in SOBS that the probability of an upper cloud, given a lower cloud, is assumed to be the same when high cloud cannot be seen (because lower cloud is overcast) as when it can be seen (when low cloud is present but not overcast) (Hahn et al. 1982). This assumption may overestimate high clouds and consequently cause a higher frequency of multilayered clouds. Larger discrepancies at two stations (numbers 7 and 21 in Fig. 15) are caused by lower vertical resolution (50 mb) after 1970 (see section 3).

At three Atlantic Ocean ship sites (station numbers 1 to 3 in Table 1), the frequency of single-layered clouds is 52%, consistent with the 56% value found by Tian and Curry (1989). The frequency of single-layered clouds in our dataset is much lower than that in PWR95, in which it is higher than 90% at most stations (compare Fig. 15 with Fig. 3 in PWR95).

d. Comparing latitudinal and seasonal variations with PWR95

The RAOBS data at 28 sites in the Northern Hemisphere (Table 1) are used to estimate the latitudinal and seasonal variations of cloud-top and cloud-base heights MSL and layer thicknesses over ocean. These results are compared with those in PWR95, which used a combination of only 14 island sites and 15 coastal sites to represent ocean clouds. The main features are very similar to those found in PWR95. Overall, cloud-layer thickness increases only slightly with latitude (Fig. 16, cf. Fig. 9b in PWR95). However, average cloud top and base are 1007 and 672 m higher, respectively, than those in PWR95 due to more samples of middle and high clouds. The thicknesses of middle and high clouds, which are defined by top altitudes z_t, $z_t \leqslant 3000$ m for low clouds, 3000 m $< z_t \leqslant 7600$ m for middle clouds, and $z_t > 7600$ m for high clouds, increase with latitude (Fig. 17, cf. Fig. 10b in PWR95). The much smaller layer thickness at 70°–80°N is from only one station. Similar seasonal variations are also found, such that high clouds are thinnest in summer at 40°–80°N (cf. Fig. 11b in PWR95). The amplitude of the seasonal

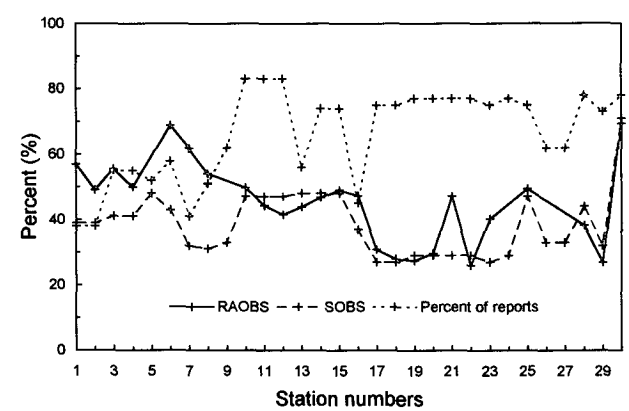

FIG. 15. Frequency of occurrence of single-layered clouds from RAOBS and SOBS at 30 sites. The dotted line is percentage of ship reports contributing to the statistics of the high-level cloud.

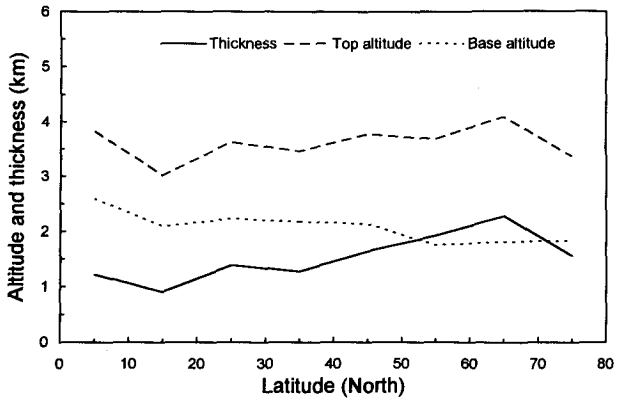

FIG. 16. Latitudinal variations of average cloud-top altitude, cloud-base altitude, and cloud-layer thickness.

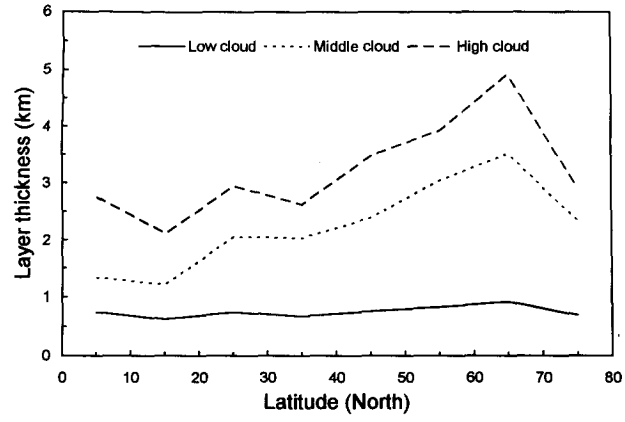

FIG. 17. Latitudinal variations of layer thicknesses of low, middle, and high clouds defined by cloud-top altitude.

variation of high cloud thicknesses at 40°–80°N, however, is about 1.5 km smaller than that in PWR95, which may be caused by the domination of coastal sites at high latitudes in PWR95. In PWR95, tropical clouds occur in three base-altitude groups (0–2, 2–6, and 6–10 km) (cf. Fig. 13 in PWR95), which are also found here (not shown). All these results suggest that the PWR95 ocean statistics are generally representative, except for the effect of undersampling upper-level clouds.

5. Preliminary statistics

To illustrate the kind of information about cloud layers that could be obtained from an analysis of the whole rawinsonde data collection, we present some preliminary statistics from our limited 30-site sample. Only the data after 1970 are employed in the statistics of frequency of multilayered clouds to avoid the vertical resolution changes around 1970. All data are used for the analysis of frequency distributions of cloud boundaries and layer separation distances since the vertical resolution change has negligible impact on them.

a. Frequency of multilayered clouds

Two or more cloud layers commonly occur simultaneously over the same location (Warren et al. 1985); however, the properties of overlapping cloud layers remain largely unexplored. We assume that two layers in the same sounding are overlapped, even though the rawinsonde is displaced by the wind by about 10–30 km during ascent, because most clouds occur as mesoscale to synoptic-scale features (Rossow and Cairns 1995). Figure 18 displays the frequencies of occurrence of single- and multilayered clouds over the 30 sites, separating the results from before and after 1970 (Fig. 18 excludes clear cases). The frequency of multilayered clouds after 1970 is 28% higher than before 1970 (Fig. 18) due to the increase of average RAOBS vertical resolution (from 50 to 30 mb). After 1970, 44% of clouds are single layered and 56% are multilayered; half of the multilayered clouds are two-layered clouds (Fig. 18).

The geographic and seasonal variations of the frequency of multilayered clouds at 25 sites are shown in Fig. 19 (only data after 1970 are used, except for station 14642 where data after 1980 are used). At the tropical stations (10°S–10°N) there are more multilayered clouds than at other stations; the least frequent multilayered clouds occur at the two subtropical eastern Pacific stations (numbers 6 and 30) (Fig. 19). The frequency of multilayered clouds is higher in summer than in winter at low latitudes. Negligible seasonal variations appear at the North Atlantic stations (numbers 1–4), but more multilayered clouds appear in winter at the two subtropical eastern Pacific stations (numbers 6 and 30). Infrequent occurrence of multilayered clouds at stations 40604 and 17 (number 21 and 7) is caused by the lower vertical resolution (50 mb) after 1970.

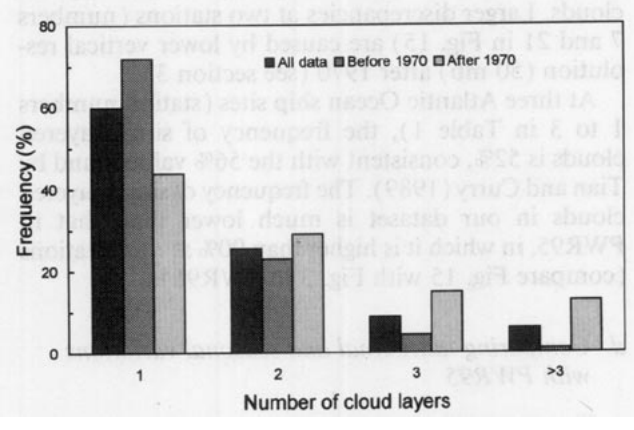

FIG. 18. The frequencies of one-, two-, three-, and more than three-layered clouds using all rawinsonde data and the data before and after 1970 at 30 sites.

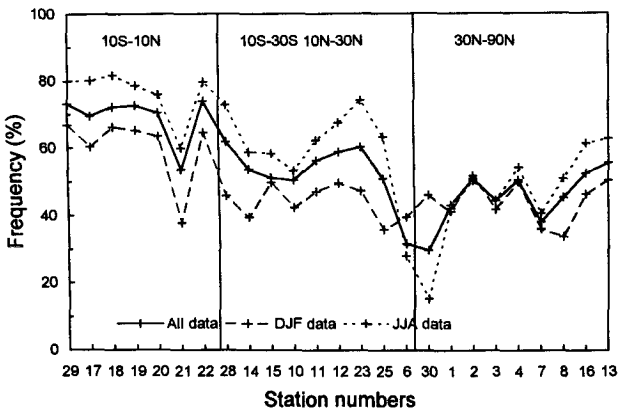

FIG. 19. The frequency of multilayered clouds at 25 stations using all data, winter month (December–February) data, and summer month (June–August) data after 1970. Station numbers correspond to the numbers shown in Table 1.

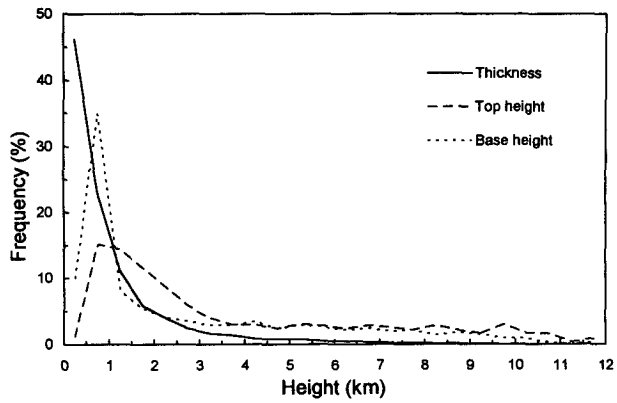

FIG. 20. Frequency distribution of cloud-base height MSL, cloud-top height MSL, and cloud-layer thickness using all data at 30 sites.

Surface observations show that over-ocean cirrus commonly overlie boundary layer convective clouds or stratus clouds (Hahn et al. 1982; Warren et al. 1985; Tian and Curry 1989). Hahn et al. (1982) show that cirrus (Ci) occur more frequently with cumulus (Cu) or cumulonimbus (Cb) cloud at low latitudes (30°S–30°N) and with stratus cloud at high latitudes. Therefore, a higher frequency of multilayered clouds is likely to be associated with the maximum frequency of occurrence of Cb and Cu in summer at low latitudes and a higher probability of Ci also being present in summer than in winter given a low convective cloud type (Cu or Cb) (Hahn et al. 1982). The small seasonal variations at high latitudes are probably due to two compensating factors: higher frequency of stratus clouds in summer (Klein and Hartmann 1993b) and more multilayered cloud systems associated with frontal activity in winter. The minimum frequency of multilayered clouds at San Nicolas Island (number 30) is likely due to the larger probability (about 40%–60%) that Ci is present alone (Warren et al. 1985). The reasons for the exceptional behaviors of multilayered cloud systems at the two subtropical eastern Pacific stations (numbers 6 and 30), which are in the Californian subtropical marine stratus region, remain unknown.

b. Frequency distribution of cloud boundaries

The frequency distributions of cloud boundaries (top and base) and layer thickness as a function of height are shown in Fig. 20. Cloud bases are located below 2 km (all heights MSL) 57% of the time with an evenly distributed low frequency above 2 km and a mean value of 2.6 km. Cloud tops occur below 3 km 54% of the time with a relatively uniform distribution above 3 km and a mean value of 3.6 km. Eighty-four percent of cloud layers tend to be thinner than 3 km with a mean thickness of 1.0 km, but clouds thicker than 3 km do occasionally exist. The distribution of cloud occurrence is similar to that of cloud top (not shown). About half of all cloud layers are below 3 km; the other half are equally distributed from 3 to 7 km. The frequency of cloud occurrence decreases with height above 7 km.

The features shown in Fig. 20 result from mixture of different cloud distributions from the 30 sites. Figure 21 displays the frequency distributions of cloud occurrence at three stations located in different climate regimes. In the tropical western Pacific (station 40308) about half of the cloudiness is located below 3 km with a peak between 0.5 and 1 km, and another half is approximately evenly distributed above 3 km. At station 14, located in the Californian marine stratus region, clouds are concentrated below 2 km, but there is a secondary mode at around 8 km. The distribution in the North Atlantic (station 2) exhibits a gradually decreasing frequency above 1.5 km.

Figure 22 shows the vertical distribution of cloud occurrence for the two-layered cloud systems. The lower layer occurs primarily below 3 km with a peak at 1 km and the higher layer occurs over a wide range

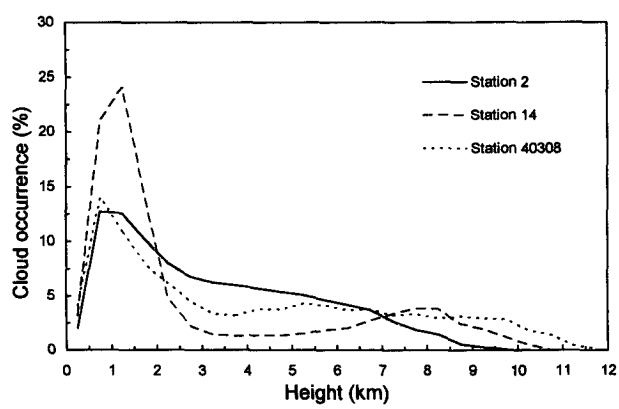

FIG. 21. Vertical frequency distributions of cloud occurrences at stations 2, 14, and 40308.

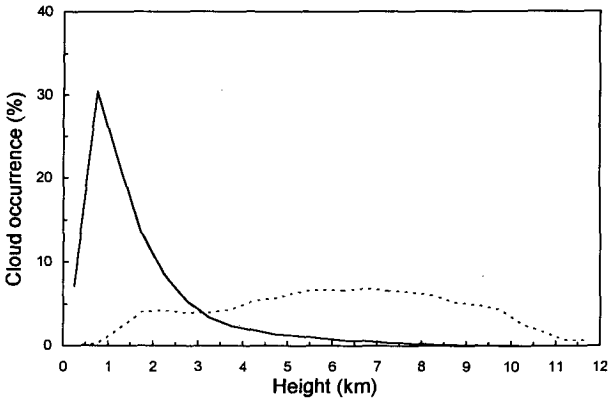

FIG. 22. Frequency distribution of cloud occurrence for a two-layered cloud system using all data at 30 sites. The solid line is for the lower layer, and the dotted line is for the higher layer.

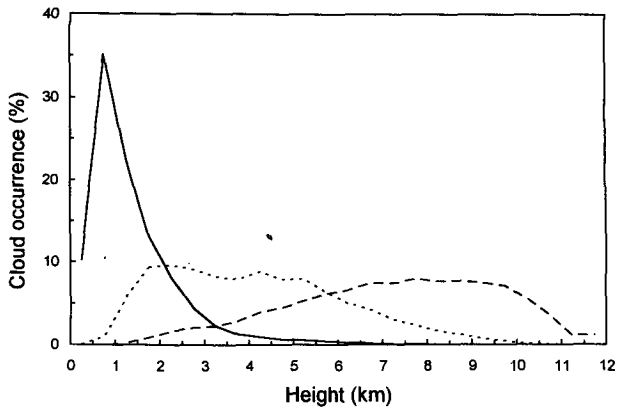

FIG. 23. As in Fig. 22 except for three-layered cloud systems. The solid line is for the lowest layer, the dotted line for middle layer, and the dashed line for the highest layer.

from 2 to 11 km with a maximum around 6 km. The lower layer is slightly thinner than the higher one (not shown), but both are about 1-km average thickness. For three-layered cloud systems, the lowest layer is still located below 3 km, the middle one from 2 to 9 km with an even distribution from 2 to 5 km, and the highest layer from 2 to 12 km with a maximum around 8.5 km (Fig. 23). There is no significant difference in layer thicknesses among the three cloud layers except that the middle layer is slightly thinner and the highest one is slightly thicker (not shown). The lowest layer of the two- and three-layered systems is almost always in the atmospheric boundary layer. Cloud top and base show the same features as cloud occurrence for both two- and three-layered cloud systems (not shown).

The vertical distribution of multilayered cloud systems also varies geographically as illustrated in Fig. 24 for two-layered clouds. The lower layer below 3 km occurs at all three stations, but the higher layer exhibits different features. The higher layer is widely distributed between 2 and 12 km at the tropical Pacific (station 40308). There is a bimodal distribution at about 2 and 8 km at the weather ship at 30°N (station 14). In the North Atlantic (station 2), the upper-layer cloud location is symmetrically distributed around 6 km.

c. *Frequency distribution of layer separation distances*

The frequency distribution of the separation distances between two consecutive layers in multilayered cloud systems is shown in Fig. 25. The separation distance has a wide range from 0.25 to 10 km with a peak frequency between 0.5 and 1 km and a mean value of 2.1 km. Thirty percent of the cases have separation distances that are smaller than average layer thickness of multilayered clouds (813 m). The separation distance also varies with the locations of the sites (see two examples in Fig. 25). A striking feature is two peaks at 1 and 6 km at the weather ship at 30°N (station 14). At station 40308, the distribution of separation distance is similar to that using all data over 30 sites (solid line in Fig. 25).

6. Summary and discussion

A revised RAOBS analysis method has been developed to use relative humidity profiles to determine cloud-top and cloud-base heights, particularly for multilayered cloud cases. The analysis method is evaluated by comparing RAOBS-determined cloud properties with similar results from surface and satellite observations. The comparison of cloud occurrence with individual SWOBS shows that RAOBS usually can detect the same number of cloud layers for low and middle clouds. RAOBS appear to miss about one-third of the high-level clouds reported by surface observers, particularly those classified as cirrus fibratus, which are highly scattered and very thin. Comparison of RAOBS-determined cloud-top pressures with ISCCP results shows

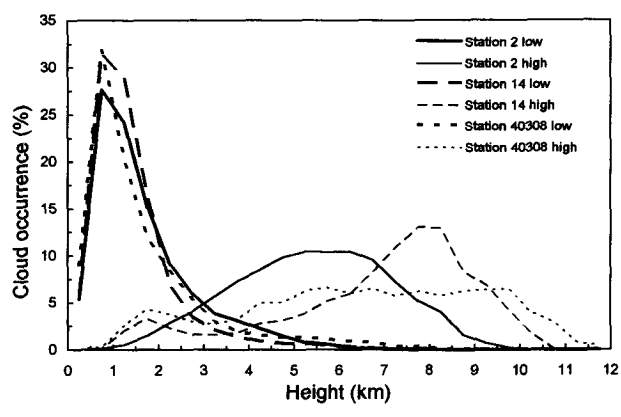

FIG. 24. Vertical frequency distribution of cloud occurrence for two-layered cloud systems at stations 2, 14, and 40308.

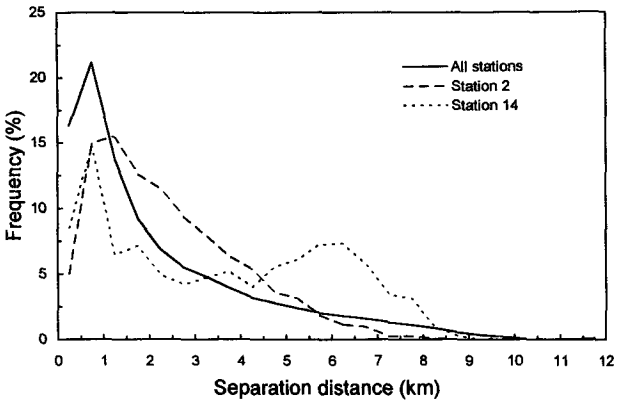

FIG. 25. Frequency distribution of the separation distance between two consecutive layers in a multilayered cloud system using all data at 30 sites and at stations 2 and 14.

good agreement for low and middle clouds, but also shows RAOBS-determined high-level cloud-top pressures to be higher than those from ISCCP. It should be remembered that ISCCP also overestimates cloud-top pressures (Liao et al. 1995b). Therefore, cirrus clouds must be severely underestimated from RAOBS.

The revised analysis method detects more multilayered clouds than the analysis method employed by PWR95 and obtains a frequency of multilayered cases that is qualitatively consistent with that estimated from surface observations (Hahn et al. 1982). However, the frequency of multilayered clouds detected from RAOBS is sensitive to the vertical resolution of the humidity profiles and must be considered as a lower limit because a significant fraction of high-level clouds are missed. Both systems may be missing the optically thinnest fraction of high-level clouds (almost one-third of the total amount, Liao et al. 1995a), indicating that both systems might underestimate the frequency of multilayered clouds.

Statistics of cloud vertical distribution from 30 oceanic sites indicate that clouds occur as single layers about 44% of the time and that multilayered cases are predominately two-layer cases. The frequency of multilayered cloudiness varies geographically and seasonally. Multilayered clouds are most frequent ($\approx$70%) in the Tropics and least frequent in the eastern subtropical Pacific. Multilayered clouds are more frequent in summer than in winter at lower latitudes, but the opposite variation appears at two subtropical stations. The vertical distributions of cloud tops, bases, and cloud occurrence all show a preponderance of low-level cloudiness (exaggerated somewhat by the poorer performance of RAOBS at the highest levels). The lowest cloud layer is usually located in or at the top of the atmospheric boundary layer. Average cloud layer thicknesses are about 0.8 km with a typical separation distance of 2.1 km between layers in multilayered cases.

These results are sufficiently encouraging to warrant processing the whole RAOBS collection to obtain a nearly global look at cloud vertical structure and its large-scale variation with location and season. A more accurate description of high-level clouds may require combining the RAOBS and satellite results, however. Further study of the satellite results for high-level clouds is still needed.

Acknowledgments. This work was supported by NSF ATM-9110536 (TOGA COARE) and the NASA Global Change Model and Data Assessment Program. We thank Dr. Roy Jenne at NCAR for supplying the rawinsonde dataset, Dr. Tony DelGenio for useful suggestions, and Alison Walker for computer assistance.

REFERENCE

Ansmann, A., and Coauthors, 1993: Lidar network observation of cirrus morphological and scattering properties during the International Cirrus Experiment 1989: The 18 October 1989 case study and statistical analysis. *J. Appl. Meteor.*, **32**, 1608–1622.

AWS, 1979: The use of the skew of T, log P diagram in analysis and forecasting. Air Weather Service Tech. Rep., AWS/TR-79/006, Scott AFB, IL, 150 pp.

Brest, C. L., and W. B. Rossow, 1992: Radiometric calibration and monitoring of NOAA AVHRR data for ISCCP. *Int. J. Remote Sens.*, **13**, 235–273.

Bunker, A. F., 1953: On the determination of moisture gradients from radiosonde records. *Bull. Amer. Meteor. Soc.*, **34**, 406–409.

Collins, W. G., and L. S. Gandin, 1990: Comprehensive hydrostatic quality control at the National Meteorological Center. *Mon. Wea. Rev.*, **118**, 2752–2767.

Curry, J. A., C. D. Ardeel, and L. Tian, 1990: Liquid water content and precipitation characteristics of stratiform clouds as inferred from satellite microwave measurements. *J. Geophys. Res.*, **95**, 16 695–16 671.

Elliott, W. P., and D. J. Gaffen, 1991: On the utility of radiosonde humidity archives for climate studies. *Bull. Amer. Meteor. Soc.*, **72**, 1507–1520.

Essenwanger, O., and G. H. Haggard, 1962: Frequency of clouds in height layers for Berlin (Tempelhof). *J. Appl. Meteor.*, **1**, 560–569.

Feigelson, E. M., 1978: Preliminary radiation model of a cloudy atmosphere. Part I: Structure of cloud and solar radiation. *Beitr. Phys. Atmos.*, **51**, 203–229.

Gaffen, D. J., 1993: Historical changes in radiosonde instruments and practices final report. WMO/TD-No. 541, Instruments and Observing Methods Report No. 50, 123 pp.

——, T. P. Barnett, and W. P. Elliott, 1991: Space and time scales of global tropospheric moisture. *J. Climate*, **4**, 989–1008.

Garand, L., C. Grassotti, J. Halle, and G. L. Klein, 1992: On differences in radiosonde humidity-reporting practices and their implications for numerical weather prediction and remote sensing. *Bull. Amer. Meteor. Soc.*, **73**, 1417–1423.

Hahn, C. J., S. G. Warren, J. Gordon, R. M. Chervin, and R. Jenne, 1982: Atlas of simultaneous occurrence of different cloud types over ocean. NCAR Tech. Note TN-201 + STR, 212 pp.

——, ——, ——, ——, and ——, 1984: Atlas of simultaneous occurrence of different cloud types over land. NCAR Tech. Note TN-241 + STR, 211 pp.

Heymsfield, A. J., 1993: Microphysical structures of stratiform and cirrus clouds. *Aerosol-Cloud-Climate Interactions*, P. V. Hobbs, Ed., International Geophysics Series, Vol. 54, Academic Press, 97–121.

Hobbs, P. V., and A. L. Rangno, 1985: Ice particle concentrations in clouds. *J. Atmos. Sci.*, **42**, 2523–2549.

Houze, R. A., 1982: Cloud clusters and large-scale vertical motions in the tropics. *J. Meteor. Soc. Japan*, **60**, 396–410.

Klein, S. A., and D. L. Hartmann, 1993a: Spurious trend in the ISCCP C2 data set. *Geophys. Res. Lett.*, **20**, 455–458.

——, and ——, 1993b: The seasonal cycle of low stratiform clouds. *J. Climate*, **6**, 1587–1606.

Liao, X., W. B. Rossow, and D. Rind, 1995a: Comparison between SAGE II and ISCCP high-level clouds. Part I: Global and zonal mean cloud amounts. *J. Geophys. Res.*, **100**, 1121–1135.

——, ——, and ——, 1995b: Comparison between SAGE II and ISCCP high-level clouds. Part II: Locating cloud tops. *J. Geophys. Res.*, **100**, 1137–1147.

Minnis, P., P. W. Heck, and D. F. Young, 1993: Inference of cirrus cloud properties using satellite-observed visible and infrared radiances. Part II: Verification of theoretical cirrus radiative properties. *J. Atmos. Sci.*, **50**, 1305–1322.

Oort, A. H., 1983: Global atmospheric circulation statistics, 1958–1973. NOAA professional paper 14, 180 pp.

Poore, K., J. Wang, and W. B. Rossow, 1995: Cloud layer thicknesses from a combination of surface and upper-air observations. *J. Climate*, **8**, 550–568.

Pratt, R. W., 1985: Review of radiosonde humidity and temperature errors. *J. Atmos. Oceanic Technol.*, **2**, 404–407.

Randall, D. A., Harshvardhan, D. A. Dazlich, and T. G. Corsetti, 1989: Interactions among radiation, convection, and large-scale dynamics in a general circulation model. *J. Atmos. Sci.*, **46**, 1943–1970.

Rossow, W. B., and R. A. Schiffer, 1991: ISCCP cloud data products. *Bull. Amer. Meteor. Soc.*, **72**, 2–20.

——, and B. Cairns, 1995: Monitoring changes of clouds. *Clim. Change*, in press.

Rossow, W. B., L. C. Garder, P-J. Lu, and A. Walker, 1991: International Satellite Cloud Climatology Project (ISCCP) documentation of cloud data. WMO-TD-No. 266 (revised), World Climate Research Program (ICSU and WMO), 76 pp.

Sassen, K., D. Starr, and T. Uttal, 1989: Mesoscale and microscale structure of cirrus clouds: Three case studies. *J. Atmos. Sci.*, **46**, 371–396.

Schwartz, B. E., and C. A. Doswell III, 1991: North American rawinsonde observations: Problems, concerns, and a call to action. *Bull. Amer. Meteor. Soc.*, **72**, 1885–1896.

Slingo, A., and J. M. Slingo, 1988: The response of a general circulation model to cloud longwave radiative forcing. Part I: Introduction and initial experiments. *Quart. J. Roy. Meteor. Soc.*, **114**, 1027–1062.

Starr, D. O., and S. K. Cox, 1980: Characteristics of middle and upper tropospheric clouds as deduced from rawinsonde data. Atmospheric Science paper no. 327, Department of Atmospheric Science, Colorado State University, Fort Collins, CO.

Tian, L., and J. A. Curry, 1989: Cloud overlap statistics. *J. Geophys. Res.*, **94**, 9925–9935.

Warren, S. G., C. J. Hahn, and J. London, 1985: Simultaneous occurrence of different cloud types. *J. Climate Appl. Meteor.*, **24**, 658–667.

——, ——, ——, R. M. Chervin, and R. L. Jenne, 1986: Global distribution of total cloud cover and cloud type amounts over land. NCAR Tech. Note NCAR/TN-273 + STR, 29 pp., plus 200 maps.

——, ——, ——, ——, and ——, 1988: Global distribution of total cloud cover and cloud type amounts over ocean. NCAR Tech. Note NCAR/TN-317 + STR, 42 pp., plus 170 maps.

Webster, P. J., and G. L. Stephens, 1984: Cloud-radiation interaction and the climate problem. *The Global Climate*, J. Houghton, Ed., Cambridge University Press, 63–78.